University of Birjand
Water Harvesting Research Vol. 7, No. 2, Autumn & Winter 2024, Original paper p. 301-313
10.22077/JWHR.2025.8070.1150

Assessing Annual and Seasonal Precipitation Trends in the Karun River Basin Using Co-Kriging: An Over 60-Year Analysis

Amin Khoramian[a&*]

[a]Assistant Professor, Department of Hydrology and Water Resources, Shahid Chamran University of Ahvaz, Ahvaz, Iran.

[*]Corresponding Author, E-mail address: a.khoramian@scu.ac.ir
Received: 26 August 2024/ **Revised**: 06 January 2025/ **Accepted**: 08 January 2025

Abstract

The Karun River Basin is an important source of water in Iran, located in a semi-arid region that is under increasing pressure due to changing precipitation patterns. In this work, the trends of precipitation from 1955 to 2019 at 163 meteorological and synoptic stations in the Karun River basin were investigated using the Co-Kriging method to generate precipitation maps for the study period. Although there is no trend in annual precipitation from 1955 to 2019, there is a statistically significant decreasing annual trend at the 10% significance level in the period from 1985 to 2019; -6.6 is the negative slope coefficient. This could indicate a shift towards drier conditions in the latter part of the study period, which affects the availability and management of water resources. The seasonal trends are opposite: a possible decrease in winter precipitation with a slope coefficient of -0.102, indicating drier winters, and a possible increase in fall precipitation, where the slope coefficient is positive at 0.131, indicating wetter autumns. Even though these seasonal trends are not statistically significant with p-values of 0.226 and 0.099, respectively, they underline the complex and dynamic nature of precipitation patterns in the catchment. It is therefore very important to understand the trends of current water resource management strategies and possible future changes in the region to avert the associated risks to irrigated agriculture, domestic water supply, and flood control in this important area.

Keywords: Co-Kriging, Karun, Precipitation, Seasonal patterns, Trend analysis

1. Introduction

The occurrence of precipitation is an important part of the hydrological cycle and a decisive factor for the availability and natural management of water resources. One of the most important ways in which the long-term variability of climate can be determined is the trend in precipitation, for which the potential impact on the water yield of river basins should be assessed. This has demonstrated the variability of precipitation in the Karun River basin, a major water source in Iran, which highlights the need to access and wisely manage available water resources (Boroujerdy, 2008; Jamali et al., 2022). Numerous studies have been conducted in Iran (Asakereh et al., 2025; Darand and Pazhoh, 2022) and the Karun river basin (Farhangi et al., 2016; Halabian, 2019; Saeidi et al., 2024) to analyze precipitation trends using different methods and time periods. This study investigated the time series variations of annual and seasonal precipitation trends in the said catchment using Co-Kriging over a period of 60 years.

In addition, the general precipitation of previous studies indicated that there was an increasing trend in the northern Karun watershed over the last 50 years, in addition to huge seasonal and stationary variations (Farsani et al., 2013). The Izeh station in Khuzestan province also showed a downward trend in the major precipitation indices in the

period from 1990 to 2010 (Khalili et al., 2014). In addition, the studies over the past 50 years have shown the trend of irregularities and concentrations in precipitation in the Karun River basin, indicating the complex nature of precipitation trends in the region (Khalili et al., 2016). In addition, a study indicated an increasing precipitation trend for the wettest month in the southwestern semi-arid region of Iran, including the Karun river basin (Pour et al., 2020). In 2017, methods of Kriging interpolation were used in research in this regard (Javari, 2017). In this sense, spatial interpolation techniques obviously help to understand precipitation patterns. On the other hand, statistical refinements of these series have been structured to improve precipitation attributes in the Karun basin, such as that of Yazdandoost et al. (2023). Consequently, statistics have the potential to be used in improving precipitation forecasts.

Long-term data have therefore become key to understanding precipitation trends in the country, as some studies aim to analyze the temporal variability of precipitation in Iran during the period 1966–2005 (Tabari et al., 2011). In addition, divergent trends in precipitation have been observed in different parts of Iran: They decreased in the west, northwest and southeast, which had a negative impact on the Karun River basin and underlined the need for region-specific analysis (Boroujerdy, 2008). The negative trend in extreme precipitation events in the regions with decreasing mean annual precipitation and low precipitation, such as in Karun, due to high temperatures, has become noticeable, underlining the link between climate change and precipitation patterns (Jamali et al, 2022). Mosaffa et al. (2020) analyzed precipitation trend in Iran over 1983-2018 period using PERSIANN-CDR estimates. They found that Zagros Mountains located at the upstream of Karun river basin experiencing an upward trend in summer and fall seasons.

This paper aims to fill existing gaps in the literature by analyzing both annual and seasonal precipitation trends over a comprehensive period of more than 60 years using the Co-Kriging method. This innovative approach not only captures the spatial variability of precipitation but also enables a detailed examination of seasonal variations, which have been largely overlooked in previous studies. Unlike earlier research that often concentrates on narrow timeframes or specific locations, this study provides a holistic view of the changing precipitation patterns in the Karun River basin. The findings will be crucial for informing water resource management strategies and mitigating the impacts of climate change, particularly in light of the complex and dynamic nature of precipitation trends reported in earlier works.

2. Materials and Methods

2.1. Study area and used data

This study focuses on the catchment area of the Karun, the largest river basin in Iran, which is located in the southwest of the country. The Karun and Dez rivers originate on the western slopes of the Zagros Mountains. They then flow through the Khuzestan plain before merging and finally flowing into the Persian Gulf as the Karun. Topographically, the catchment area is very varied and includes mountainous areas, plains and a semi-arid climate, which has a strong impact on the local hydrology.

Precipitation data from 163 meteorological and synoptic stations of the Iranian Ministry of Energy and the Meteorological Organization from 1955 to 2019 were used for the present study. The Dezful Dam and Gotvand Dam stations are the oldest and date back to 1955. The Ahvaz and Shushtar stations started recording in 1956, and the Darakhzineh, Betound and Pol Shalu stations have data from 1957. All locations of these stations are shown in Figure 1.

This extensive dataset provides a suitable background for the assessment of annual and seasonal precipitation trends in the Karun catchment and allows an in-depth study of the relationships between these trends and climate variability and local environmental conditions.

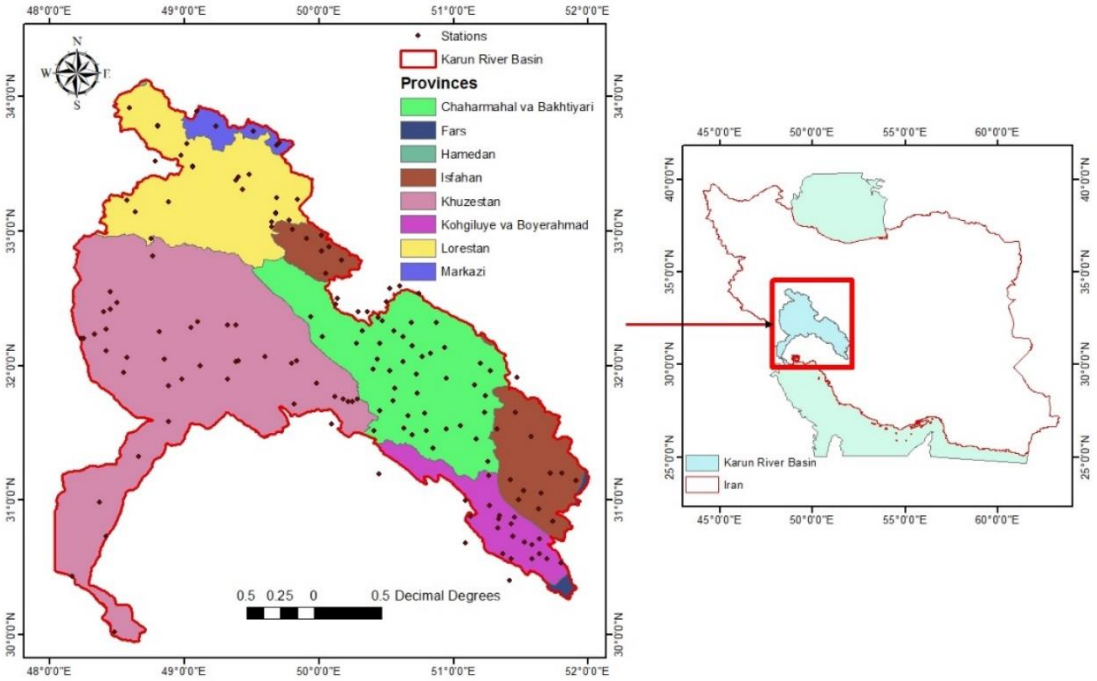

Fig. 1. Study area and location of used rain-gauge stations

2.2. Missed data filling

The HEC4 software, which is based on probabilistic regression (Hydrologic Engineering Center, 1971), was used to reconstruct the station data. This method has undeniable advantages over traditional correlation methods, which will be briefly discussed in the context of the HEC4 software. The software uses the following regression relationship:

$$Y = a + bX + z \cdot s \quad (1)$$

where Y is the data from the target station, X is the data from the reference station, a and b are regression coefficients, z is a standard normal variable (random number) and s is the standard deviation of the available data at station Y. R^2 denotes the coefficient of determination of the correlation. In this context, the component that resembles the traditional correlation represents the deterministic part of the relationship, while the other component characterizes the random aspect. In this method, the monthly data of each station is correlated with the monthly data of all stations and the previous month's data for all stations.

After reconstruction, all relationships and correlation coefficients are recalculated. In addition, a set of correlation coefficients is estimated for each reconstruction. At least $2n \times 12$ correlation coefficients are calculated, where n is the number of stations.

The selection of suitable stations for data reconstruction is based not only on the correlation (R), but also on the number of common data points between the two stations and the length of the existing data series for the target station. The following relationship is used for this purpose:

$$L_y = L_{shared} \cdot \frac{R^2}{L_x} \quad (2)$$

where L_y is the effective length of the reconstructed data series for station Y, L_{shared} is the length of the common data series at station Y, L_x is the length of the existing data series at station X and R^2 is the coefficient of determination of the correlation.

In this method, the appropriate station would be selected based on maximum L_y. If $R^2 = 1$, then L_y would equal L_{shared}, which is rarely the case. because R^2 is always less than 1. Therefore, L_y remains between L_{shared} and L_x (Hydrologic Engineering Center, 1971). Using this method, the missing values in monthly precipitation data of used stations are reconstructed in the Karun river basin.

2.3. Outlier detection

Identifying outliers is a crucial step in data analysis, as outliers can significantly distort the results and lead to misleading interpretations. Various methods have been developed to identify outlier data points, each of which has its strengths and weaknesses. Among these methods, the quality control (QC) test was selected for this study because it is reliable and easy to use (Asikoglu, 2017).

The QC test is based on the calculation of a certain test index and its comparison with a predefined threshold value. The calculation steps of this method are as follows: First, the median ($x_{0.5}$), the first quartile ($x_{0.25}$), and third quartile ($x_{0.75}$) are calculated from the data set. These measures indicate the central tendency and the dispersion of the data, which are essential for identifying outliers.

Next, the mean absolute deviation (MAD) from the median is calculated to assess the variability within the data. This step helps to quantify how much individual data points deviate from the median, giving a clearer picture of data dispersion. The test index is then calculated using the following equation:

$$index = \begin{cases} 0 & if \quad MAD = 0 \\ \dfrac{|x_i - x_{0.5}|}{(x_{0.75} - x_{0.25})} & if \quad x_{0.25} \neq x_{0.75} \\ \dfrac{|x_i - x_{0.5}|}{MAD} & else \end{cases} \tag{3}$$

where x_i represents each individual data point. The index quantifies the deviation of the individual data points from the median in relation to the variability of the data set.

Once the test index is calculated, it is compared with a predefined threshold value, which is usually 2. If the index exceeds this threshold, the corresponding data point is classified as an outlier. This threshold helps to distinguish between normal variability in the data and extreme values that may indicate measurement errors or anomalies.

The QC test was applied to the reconstructed data from all meteorological stations. All identified outlier data points were removed to ensure the integrity of the data set. The process of identifying and removing outliers was iterative. After the initial detection of outliers, the removed data points were reconstructed using the HEC4 software. The QC test was then re-applied to the newly reconstructed data set. This iterative process was continued until a data set with reconstructed data without outliers was achieved.

The detection and handling of outliers is critical to ensuring the accuracy and reliability of the analysis. Outliers can distort statistical analyses, affect trend assessments and ultimately lead to incorrect conclusions regarding precipitation patterns and environmental impacts in the Karun River Basin. By applying the QC test, this study aims to maintain a high standard of data quality, leading to more valid and reliable results in subsequent analyses. This rigorous approach increases the overall robustness of the results and ensures that the conclusions drawn from the data are based on sound statistical procedures.

2.4. Co-Kriging

Co-Kriging is an advanced geostatistical method that significantly enhances the estimation of precipitation by incorporating secondary correlated variables. This technique is particularly valuable in environmental studies, as it provides the Best Linear Unbiased Estimator (BLUE), which minimizes estimation variance among linear estimators. By utilizing additional datasets, such as temperature or humidity from nearby weather stations, Co-Kriging improves the accuracy of precipitation predictions.

The Co-Kriging estimator for a location x_0 can be expressed as:

$$\hat{Z}(x_0) = \sum_{i=1}^{n} w_i Z(x_i) + \sum_{j=1}^{m} v_j W(y_j) \tag{4}$$

In this equation, $\hat{Z}(x_0)$ represents the estimated precipitation at location x_0, while $Z(x_i)$ denotes the primary variable (precipitation) at known locations x_i.

The secondary variable, such as temperature, is represented by $W(y_j)$ at known locations y_j. The weights w_i and v_j are crucial as they are determined by minimizing

the estimation variance, which reflects the dependence between the primary and secondary variables.

The variance of the Co-Kriging estimator can be expressed as:

$$\begin{aligned} &Var\left(\hat{Z}(x_0)\right) \\ &= \sum_{i=1}^{n}\sum_{k=1}^{n} w_i w_k C_{Z,Z}(x_i, x_k) \\ &+ \sum_{j=1}^{m}\sum_{l=1}^{m} v_j v_l C_{W,W}\left(y_j, y_l\right) \\ &+ 2\sum_{i=1}^{n}\sum_{j=1}^{m} w_i v_j C_{Z,W}(x_i, y_j) \end{aligned} \quad (5)$$

where $C_{Z,Z}(x_i, x_k)$ is the covariance between the primary variable at two locations, while $C_{W,W}(y_j, y_l)$ represents the covariance between the secondary variable at two locations. The term $C_{Z,W}(x_i, y_j)$ denotes the cross-covariance between the primary and secondary variables, highlighting the interdependence that Co-Kriging leverages to improve estimates.

Choosing an appropriate covariance function is crucial for the success of Co-Kriging. Commonly used models include the exponential, Gaussian, and spherical covariance functions. For example, the exponential covariance function can be defined as:

$$C(h) = C_0\left(1 - e^{-\frac{h}{a}}\right) \quad (6)$$

In this equation, C_0 represents the sill, which is the variance when the distance is infinite, and a is the range parameter, indicating the distance over which the correlation decreases. This function helps model the spatial structure of the data, ensuring that closer observations influence the estimates more than those further away.

Co-Kriging is particularly effective for precipitation interpolation for several reasons. First, it allows for the integration of multiple data sources. In regions where direct precipitation measurements are sparse, incorporating data from related variables can provide a more comprehensive understanding of precipitation patterns. For instance, using temperature data can help capture the relationship between temperature and precipitation, as warmer conditions often lead to different precipitation behaviors.

Second, studies have demonstrated that Co-Kriging frequently outperforms ordinary Kriging, especially in heterogeneous environments where the correlation between precipitation and auxiliary variables is strong (Chilès and Delfiner, 2012). By utilizing the additional information from correlated datasets, Co-Kriging effectively reduces estimation variance, leading to more accurate predictions.

2.5. Trend analysis of annual and seasonal precipitation

Trend analysis is essential for understanding changes in precipitation patterns over time. By examining annual and seasonal trends, researchers can identify long-term shifts that may indicate climate change impacts. Linear trend analysis is a common method used to assess these trends, where a linear model is fitted to precipitation data over a specified period. The general form of the linear regression equation is:

$$Y_t = \beta_0 + \beta_1 t + \epsilon_t \quad (7)$$

In this equation, (Y_t) represents the precipitation value at time (t), (β_0) is the intercept, (β_1) is the slope indicating the trend, and (ϵ_t) is the error term. A positive slope (β_1) suggests an increasing trend in precipitation, while a negative slope indicates a decrease.

To evaluate the significance of the trend, the t-Student test is employed. This test assesses whether the slope (β_1) is significantly different from zero. The t-statistic is calculated as:

$$\mathrm{t} = \frac{\hat{\beta}_1}{SE\left(\hat{\beta}_1\right)} \quad (8)$$

where $(\widehat{\beta_1})$ is the estimated slope and $(SE(\widehat{\beta_1}))$ is the standard error of this estimate. The degrees of freedom for the t-test is $(n - 2)$, with (n) being the number of observations. The resulting p-value is determined based on the calculated t-statistic and degrees of freedom. A significance level of $(\alpha = 0.1)$ is used in this study; if the p-value is less than this threshold, the null hypothesis

(which posits no trend, ($\beta_1 = 0$)) is rejected, indicating a statistically significant trend (Pearson, 1895).

This methodology can be applied to both annual and seasonal precipitation data. For annual trends, researchers aggregate monthly or daily data to calculate yearly totals, providing clarity on long-term changes. Seasonal trends are analyzed by separating the data into distinct seasons (e.g., winter, spring, summer, fall) and applying the same linear regression approach.

For instance, trend analysis on historical precipitation records may reveal significant trends in specific seasons. A study might find a significant increasing trend in summer precipitation with a p-value of 0.03, suggesting that summer precipitation patterns are becoming more pronounced over time. In contrast, winter precipitation may show no significant trend, with a p-value of 0.12, indicating stability in winter precipitation patterns. The Mann-Kendall test was not investigated in this study as the focus was solely on linear regression, which provides clear insights into the trend slopes and their significance.

3. Results and Discussion

3.1. Precipitation maps

Using Co-Kriging method, the annual precipitation maps are derived for entire study period from 1959 to 2019. Then, long term averaged annual precipitation map is derived utilizing every year data. The derived precipitation map is given at Fig. **2**. In addition, evaluation metrics of derived maps is given in Table 1.

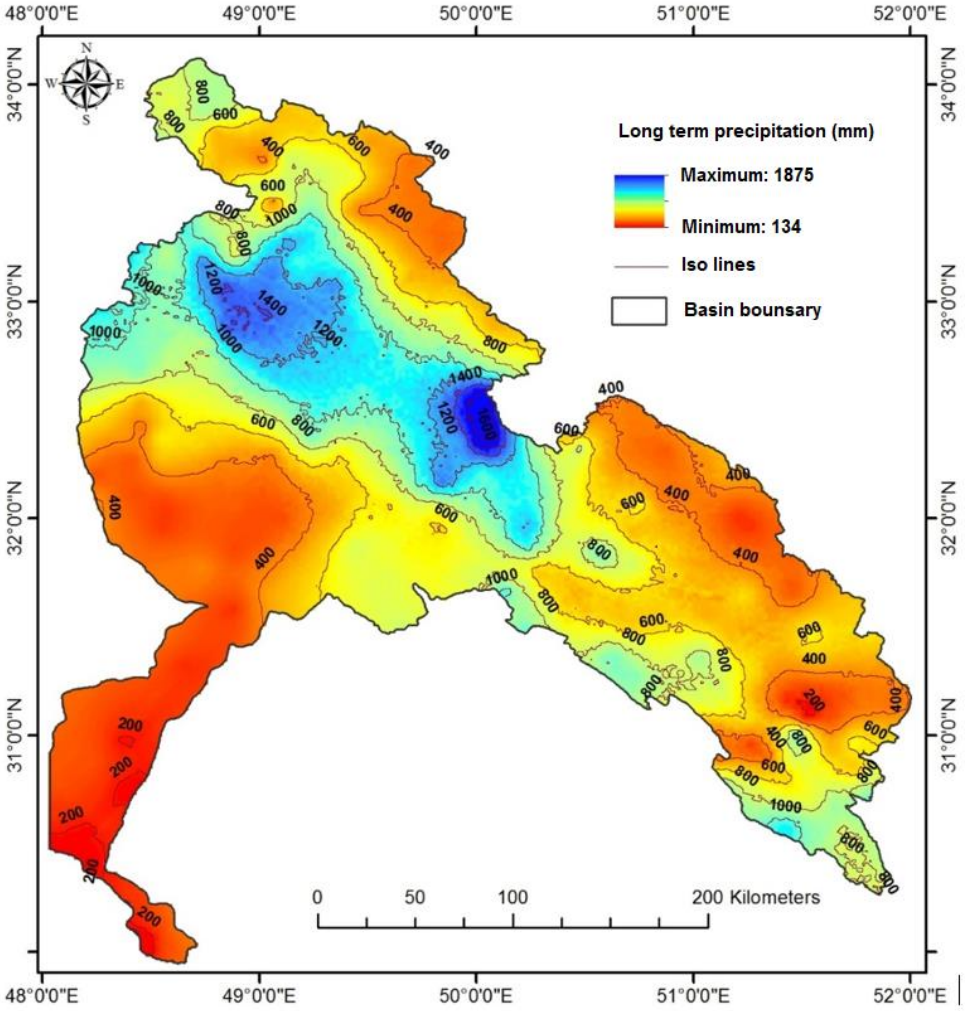

Fig. 2. Derived precipitation map for long-term period

Table 1. Evaluation metrics of derived precipitation maps

Evaluation Criteria	Equation	Value
Root of Mean Squared Error (RMSE)	$RMSE = \sqrt{\left(\frac{1}{n}\right)\sum_{n}^{i=1}(O_i - P_i)^2}$	3.72 mm
Coefficient of Determination (R^2)	$R^2 = 1 - \left(\frac{\sum_{n}^{i=1}(O_i - P_i)^2}{\sum_{n}^{i=1}(O_i - \bar{O})^2}\right)$	0.74
Bias	$\frac{1}{n}\sum_{n}^{i=1}(O_i - P_i)$	0.60 mm

Table 1 results indicate a reasonable performance of Co-Kriging method in deriving precipitation maps over study area. The Root Mean Squared Error (RMSE) of 3.72 mm shows that the model's predictions are relatively close to the observed data. A Coefficient of Determination (R^2) of 0.74 indicates that 74% of the variability in observed precipitation is explained by the derived Co-Kriging maps, reflecting a moderate fit. Additionally, the bias of 0.60 mm indicates a slight overestimation of precipitation.

Using this map, the long term averaged annual precipitation values at Dez, Karun and Great Karun river basins is calculated (Table 2). In addition, these values in every province that is located at Karun river basin is derived (Fig. **3**a). By multiplying these values and the area of every province at Karun river basin, the precipitation volume is calculated. The results are given in Fig. **3**b.

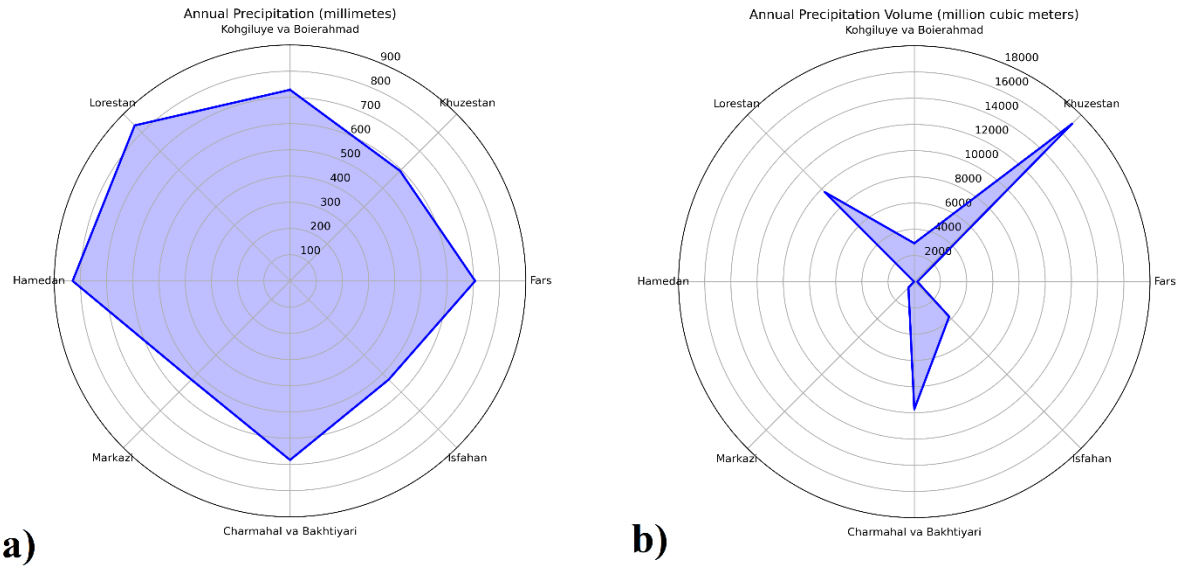

Fig. 3. Radar chart of annual precipitation in millimeters (a) and precipitation volumes in million cubic meters (b) of provinces located in Karun River Basin

Table 2. Long-Term average precipitation, basin area, and precipitation volume for the Dez, Karun, and Great Karun Basins

Basin	Long-Term Average Precipitation (mm)	Area (km^2)	Precipitation Volume (Million m^3)
Dez	757.7	23,182	17,566
Karun	602.5	43,924	26,463
Great Karun	656.6	67,106	44,063

Table 2 results show that the province with the highest annual precipitation is Lorestan, recording 838.8 mm on average. This is closely followed by Hamedan at 830.0 mm. These two northwestern provinces appear to be the wettest regions, likely due to their mountainous terrain and proximity to the Zagros mountain range. In contrast, the central provinces of Isfahan and Markazi have the lowest annual precipitation at 532.4 mm each, indicating a more arid climate in the interior of the country.

When looking at the total precipitation volume, Khuzestan emerges as the province receiving the highest amount at 17,049.8 million cubic meters annually. This is likely a function of both its high precipitation levels (593.8 mm) as well as its large geographic area. The runner-up in terms of total precipitation volume is Chaharmahal and Bakhtiari at 9,731.0 million cubic meters.

Interestingly, while Hamedan has the second highest precipitation levels, its total volume is only 16.8 million cubic meters due to its relatively small size. Conversely, the large area of Khuzestan results in a very high total precipitation volume despite its precipitation levels being lower than the wettest provinces.

Fig. **4** shows the monthly distribution of precipitation elevation in different provinces. The results show that most of precipitation occurs between September to October in all of the provinces.

One of the key observations from Fig. **4** is the significant differences in the annual precipitation totals among the provinces. The Hamedan province, with an annual precipitation of 830.0 mm, receives the highest amount of precipitation, while the Isfahan and Markazi provinces have the lowest annual precipitation at 532.4 mm. This spatial variability is likely influenced by factors such as elevation, proximity to mountain ranges, and regional climatic conditions.

During the winter months of December through February, the Kohgiluyeh and Boyer-Ahmad, Khuzestan, and Fars experience the highest levels of precipitation, with monthly totals exceeding 120 millimeters. Hamedan and Lorestan also exhibit substantial winter precipitation, with monthly averages around 100-135 millimeters. In contrast, the regions of Isfahan, Markazi, and Chaharmahal and Bakhtiari receive relatively lower, though still significant, winter precipitation, ranging from 65 to 95 millimeters per month.

The spring months of March through May continue to see high precipitation levels, though generally lower than the winter season. Hamedan and Lorestan maintain their status as the wettest regions, with spring totals around 100-150 millimeters per month. Other provinces, such as Kohgiluyeh and Boyer-Ahmad, Khuzestan, and Chaharmahal and Bakhtiari, also experience substantial spring precipitation, in the 90-110 millimeter per month range. The drier regions of Isfahan and Markazi receive 50-95 millimeters of precipitation per month during the spring.

The summer months of June through August, however, witness a dramatic drop in precipitation across all provinces. Most areas receive less than 5 millimeters of rain per month during this period, with some regions like Isfahan, Markazi, and Chaharmahal and Bakhtiari experiencing less than 1 millimeter per month. The wettest summer provinces are

Kohgiluyeh and Boyer-Ahmad, Khuzestan, and Lorestan, which still only see around 1-2 millimeters of rain per month.

Precipitation begins to increase again during the fall months of September through November, though the levels remain much lower than the winter and spring seasons. Hamedan and Lorestan continue to be the wettest regions, receiving 15-100 millimeters of precipitation per month. Other provinces like Kohgiluyeh and Boyer-Ahmad, Khuzestan, and Chaharmahal and Bakhtiari has 5-60 millimeters of fall precipitation, while the drier regions of Isfahan, Markazi, and Fars receive less than 15 millimeters per month.

3.2. Trend Analysis

To analyze annual and seasonal precipitation trends, linear regression analysis was employed using the annual precipitation data obtained in the previous section. The slope coefficients were extracted to quantify the trend, and a t-test was used to assess the statistical significance of the trends.

3.2.1. Annual Trend Analysis

To investigate the trend in annual precipitation, a trend analysis was conducted over six 14-year periods. These periods encompassed the water years 1955-1956 to 2018-2019, 1965-1966 to 2018-2019, 1975-1976 to 2018-2019, 1985-1986 to 2018-2019, 1995-1996 to 2018-2019, and 2005-2006 to 2018-2019. The slope coefficients of the trend lines were compared across these periods. Figure 5 illustrates the trend lines, while Table 3 presents the corresponding slope coefficients, significance statistics, and confidence intervals.

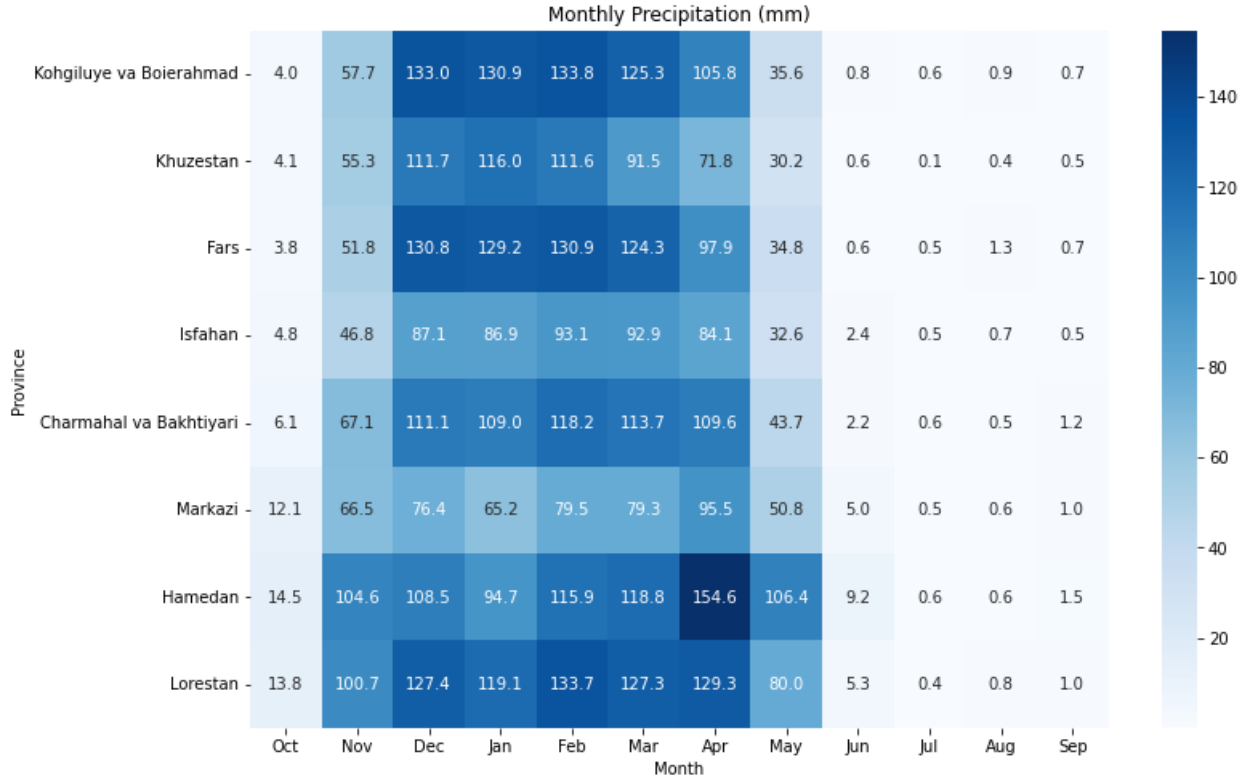

Fig. 4. Monthly Precipitation Heatmap for Provinces located in Karun river basin

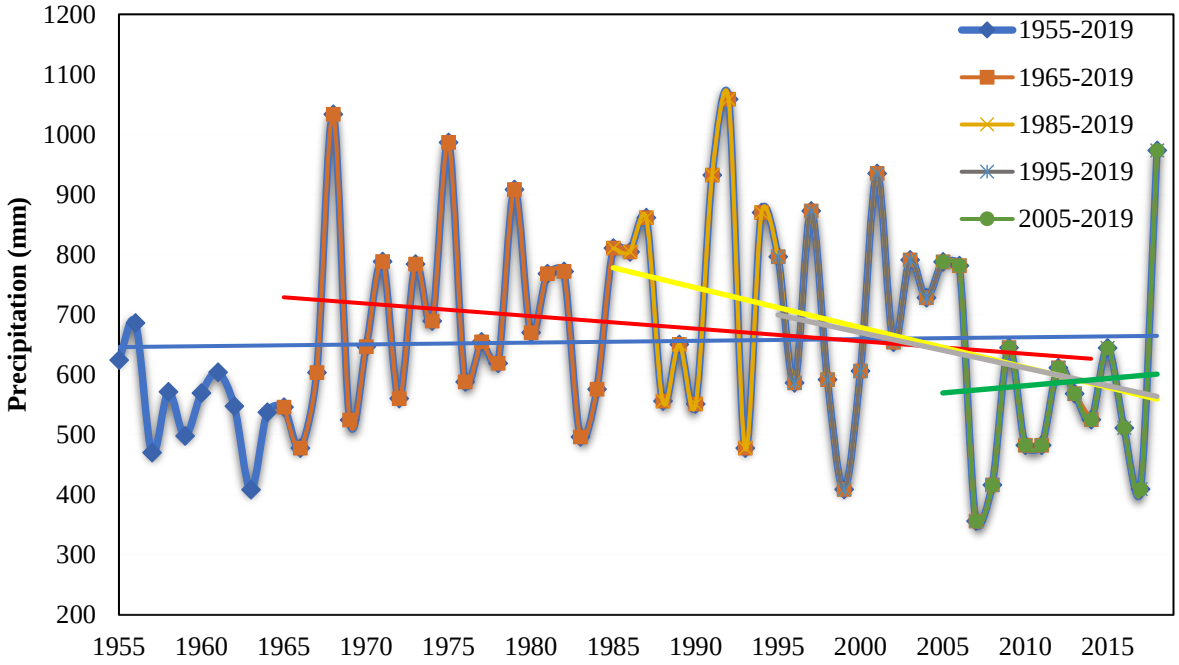

Fig. 5. Trend lines of annual precipitation in the Karun River Basin, analyzed in six 14-year periods

Table 3. Estimated slope coefficients, significance levels, and confidence intervals for linear regression trend analysis of annual precipitation in the Karun River Basin

Period	Parameter	Coefficient	t-Statistic	P-value	Lower 95% CI	Upper 95% CI
1955-1956 to 2018-2019	Intercept	250	0.2	0.9	-2868.2	3368.2
	Slope	0.3	0.3	0.8	-2	2.6
1965-1966 to 2018-2019	Intercept	3351.8	1.6	0.1	-773	7476.5
	Slope	-2	-1.3	0.2	-5	1.1
1975-1976 to 2018-2019	Intercept	6382.1	2.3	0	785.1	11979.1
	Slope	-4.1	-2.1	0	-8.2	-0.1
1985-1986 to 2018-2019	Intercept	9823.6	2.3	0	1283.2	18364
	Slope	-6.6	-2.2	0	-12.8	-0.4
1995-1996 to 2018-2019	Intercept	8808.3	1.3	0.2	-5599	23215.6
	Slope	-5.9	-1.2	0.3	-16.3	4.5
2005-2006 to 2018-2019	Intercept	-2769.8	-0.2	0.9	-38457.1	32917.5
	Slope	2.4	0.2	0.8	-23.3	28.1

Table 3 presents the results of linear regression trend analyses for annual precipitation in the Karun River Basin over six 14-year periods, covering the period from 1955-1956 to 2018-2019. The analysis reveals a complex pattern of precipitation trends with varying magnitudes and significance levels across the different periods.

The most notable finding is the presence of statistically significant decreasing trends in annual precipitation for the periods 1975-1976 to 2018-2019, 1985-1986 to 2018-2019, and 1995-1996 to 2018-2019. The slope coefficients for these periods indicate a consistent decline in precipitation, with the strongest negative trend observed during 1985-1986 to 2018-2019 (-6.6 mm/year). This suggests a potential shift towards drier conditions within the Karun River Basin during these periods. The periods 1955-1956 to 2018-2019 and 1965-1966 to 2018-2019 exhibit less conclusive trends. While the slope coefficients suggest a slight increase in precipitation during 1955-1956 to 2018-2019, the p-value indicates that this trend is not statistically significant. Similarly, the negative trend observed during 1965-1966 to 2018-2019 is not statistically significant, suggesting

that the observed changes may be due to random fluctuations.

3.2.2. Seasonal Precipitation Trend Analysis

To assess seasonal precipitation trends, the amount of precipitation in each season and its percentage of the corresponding water year were calculated for the period 1955-1956 to 2018-2019. Trend analysis was then conducted for each season using the calculated values. Fig. **6** illustrates the trends in seasonal precipitation. Table 4 presents the slope coefficients, significance statistics, and confidence intervals for the seasonal precipitation percentages.

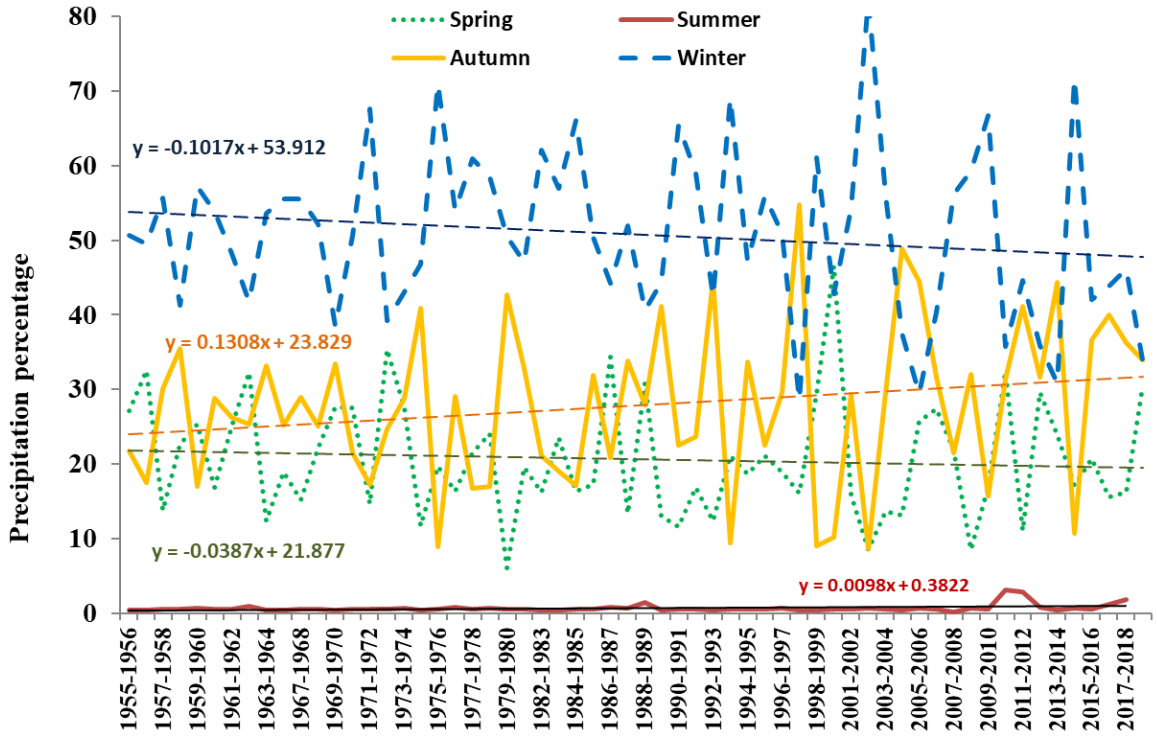

Fig. 6. Trends in seasonal precipitation percentages in the Karun River Basin

Table 4. Estimated slope coefficients, significance levels, and confidence intervals for linear regression trend analysis of seasonal precipitation in the Karun River Basin

Season	Parameter	Coefficient	t-Statistic	P-value	Lower 95% CI	Upper 95% CI
Spring	Intercept	21.877	10.615	0	17.752	26.003
	Slope	-0.039	-0.659	0.513	-0.156	0.079
Summer	Intercept	0.382	3.097	0.003	0.135	0.628
	Slope	0.01	2.724	0.009	0.003	0.017
Autumn	Intercept	23.829	8.718	0	18.358	29.3
	Slope	0.131	1.679	0.099	-0.025	0.287
Winter	Intercept	53.912	18.493	0	48.076	59.747
	Slope	-0.102	-1.223	0.226	-0.268	0.065

Table 4 presents the results of linear regression trend analyses for seasonal precipitation percentages in the Karun River Basin over the period 1955-1956 to 2018-2019. The analysis reveals distinct trends in precipitation patterns across the four seasons, highlighting potential shifts in the hydrological regime of the region.

The most notable finding is the statistically significant increasing trend in summer precipitation. The positive slope coefficient (0.010) and the low p-value (0.009) indicate a consistent increase in summer precipitation over the study period. This trend suggests a potential shift towards wetter summers in the Karun River Basin, which could have

implications for water resource management, agricultural practices, and flood risk. While the trend analysis for spring and autumn precipitation reveals some interesting patterns, the results are not statistically significant. The negative slope coefficient for spring (-0.039) suggests a potential decrease in precipitation, but the high p-value (0.513) indicates that this trend is not statistically significant. Similarly, the positive slope coefficient for autumn (0.131) suggests a potential increase in precipitation, but the p-value (0.099) is above the typical significance threshold. Further investigation with a longer time series or a more detailed analysis may be needed to confirm these trends. The analysis for winter precipitation shows a negative slope coefficient (-0.102), suggesting a potential decreasing trend. However, this trend is not statistically significant (p-value = 0.226). While the lack of significance suggests that the observed changes may be due to random fluctuations, it warrants further investigation to determine if there is a long-term shift towards drier winters in the Karun River Basin.

4. Conclusion

This study investigated the trends in annual and seasonal precipitation patterns within the Karun river basin, Iran, using a comprehensive dataset of precipitation data from 163 meteorological and synoptic stations spanning the period from 1955 to 2019. By employing a robust methodology that included data reconstruction using HEC4 software, outlier detection through the Quality Control test, and spatial interpolation using Co-Kriging, this research aimed to provide a reliable and detailed analysis of precipitation trends in the region.

The application of the Co-Kriging method played a crucial role in enhancing the accuracy of precipitation estimates by leveraging altitude and spatial correlations among the meteorological stations. The evaluation of the Co-Kriging results indicated a Root Mean Squared Error (RMSE) of 3.72 mm, a Coefficient of Determination (R^2) of 0.74, and a bias of 0.60 mm. These metrics demonstrate the effectiveness of Co-Kriging in providing reliable precipitation data.

The analysis of annual precipitation trends revealed a statistically significant decreasing trend over the study period, with a negative slope coefficient of -6.6. This finding suggests a potential long-term decline in overall precipitation in the Karun River Basin, which could have significant implications for water resources and ecological systems in the region.

The examination of seasonal precipitation trends revealed notable shifts in precipitation patterns, particularly in winter and autumn. The analysis for winter precipitation showed a potential decreasing trend, with a negative slope coefficient of -0.102. While this trend was not statistically significant (p-value = 0.226), the negative slope suggests a possible shift towards drier winters in the Karun River Basin, which could exacerbate water scarcity during the dry season and impact water resource management strategies. Conversely, the analysis for autumn precipitation revealed a potential increasing trend, with a positive slope coefficient of 0.131. Although this trend was not statistically significant (p-value = 0.099), the positive slope suggests a possible shift towards wetter autumns in the Karun River Basin, which could have implications for agricultural practices and flood risk management. While the trends in spring precipitation exhibited some interesting patterns, they were not statistically significant, requiring further investigation with a longer time series or more detailed analysis.

These findings show the complex and dynamic nature of precipitation patterns in the Karun River Basin, emphasizing the need for a comprehensive understanding of the underlying drivers of these trends. Further research is crucial to investigate the potential contributions of climate change, land-use changes, and other factors to the observed trends. Moreover, exploring the spatial variability of seasonal precipitation trends within the basin would provide a more comprehensive understanding of the hydrological changes occurring in the region.

5. Disclosure Statement

No potential conflict of interest was reported by the authors

6. References

Asakereh, H., Masoodian, S. A., Raispour, K., & Tarkarani, F. (2025). A comprehensive analysis of tempo—spatial changes in Iran's precipitation. *Theoretical and Applied Climatology*, *156*(1), 1-19.

Asikoglu, O. (2017). Outlier detection in extreme value series. *neural networks*, *4*(5).

Boroujerdy, P. K. (2008, February). The analysis of precipitation variation and quantiles in Iran. In *Proceedings of the 3rd IASME/WSEAS International Conference on Energy & Environment, University of Cambridge, UK* (pp. 248-53).

Chiles, J. P., & Delfiner, P. (2012). *Geostatistics: modeling spatial uncertainty* (Vol. 713). John Wiley & Sons.

Darand, M., & Pazhoh, F. (2022). Spatiotemporal changes in precipitation concentration over Iran during 1962–2019. *Climatic Change*, *173*(3), 25.

Farhangi, M., Kholghi, M., & Chavoshian, S. A. (2016). Rainfall trend analysis of hydrological subbasins in Western Iran. *Journal of Irrigation and Drainage Engineering*, *142*(10), 05016004.

Farsani, P. A., Roshan, M. H., Vabazade, G., & Solaimani, K. (2013). Investigation of the variation trends of precipitation in last 50 year in northern Karoon watershed of Iran. *Int. J. Agric. Sci. Res.*, *3*, 317-329.

Goovaerts, P. (1997). *Geostatistics for natural resources evaluation* (Vol. 483). Oxford University Press.

Halabian, A. H. (2019). Trend analysis of extreme precipitation indices over Karoon basin using APHRODITE girdded data. *Geography (Regional Planning)*, *9*(34), 125-138.

Jamali, M., Gohari, A., Motamedi, A., & Haghighi, A. T. (2022). Spatiotemporal changes in air temperature and precipitation extremes over Iran. *Water*, *14*(21), 3465.

Javari, M. (2017). Simulation of precipitation variations in Iran using Kriging interpolation methods. *International Journal of Physical Sciences*, *12*(15), 175-183.

Khalili, K., Nazeri Tahrudi, M., & Khanmohammadi, N. (2014). Trend analysis of precipitation in recent two decades over Iran. *J Appl Environ Biol Sci*, *4*(1s), 5-10.

Khalili, K., Tahoudi, M. N., Mirabbasi, R., & Ahmadi, F. (2016). Investigation of spatial and temporal variability of precipitation in Iran over the last half century. *Stochastic environmental research and risk assessment*, *30*, 1205-1221.

Mosaffa, H., Sadeghi, M., Hayatbini, N., Afzali Gorooh, V., Akbari Asanjan, A., Nguyen, P., & Sorooshian, S. (2020). Spatiotemporal variations of precipitation over Iran using the high-resolution and nearly four decades satellite-based PERSIANN-CDR dataset. *Remote Sensing*, *12*(10), 1584.

Pearson, K. (1895). VII. Note on regression and inheritance in the case of two parents. *proceedings of the royal society of London*, *58*(347-352), 240-242.

Pour, S. H., Wahab, A. K. A., & Shahid, S. (2020). Spatiotemporal changes in precipitation indicators related to bioclimate in Iran. *Theoretical and Applied Climatology*, *141*, 99-115.

Saeidi, D., Gandomkar, A., & Nasri, M. (2024). Analyzing Trends and Exploring the Correlation Between Runoff and Precipitation in the Armand River Basin. *Sustainable Earth Trends*, *4*(1), 12-28. doi: 10.48308/ser.2024.234857.1039

Tabari, H., & Talaee, P. H. (2011). Temporal variability of precipitation over Iran: 1966–2005. *Journal of Hydrology*, *396*(3-4), 313-320.

US Army Corps of Engineers. (1971). HEC-4 monthly streamflow simulation.

Yazdandoost, F., Zakipour, M., & Izadi, A. (2023). Statistical refinement of the North American Multi-Model Ensemble precipitation forecasts over Karoon basin, Iran. *Journal of Water and Climate Change*, *14*(8), 2517-2530.

© 2024 by the Authors, Published by University of Birjand. This article is an open access article distributed under the terms and conditions of the Creative Commons Attribution 4.0 International (CC BY 4.0 license) (http://creativecommons.org/licenses/by/4.0/).